CONSTANT FREQUENCY HYSTERESIS CONTROLLER IMPLEMENTATION FOR ACTIVE FILTERING SYSTEMS

BY

CONSTANTIN VLAD SURU[*], MIHAELA POPESCU and CRISTINA ALEXANDRA PREDA

University of Craiova
Faculty of Electrical Engineering

Abstract. The aim of this paper is the implementation and validation of a constant frequency hysteresis controller. This type of controller can be an alternative both to the classical hysteresis controller and proportional-integrative controller because, in theory, it can give constant switching frequency with the performances and simplicity of the hysteresis controller. The constant switching frequency hysteresis controller is a compromise between the two classical solutions. It can be obtained by combining the hysteresis comparators with the PWM suboptimal modulator. The obtained performances, on the other hand, are less good than the classical regulators corresponding performances as confirmed both by simulation and experimental. More exactly, the obtained performances are dependent by the compensating capacitor voltage controller parameters and working voltage value. It was proven, that the inverter is working at constant switching frequency, but the proposed regulator introduces a delay between the prescribed and obtained filter current. The regulator implementation was investigated on a complete active filtering system implemented in Matlab Simulink, and on an experimental setup based on the dSpace DS1103 control board.

Key words: active filter; control methods for electrical systems; power quality; Pulse Width Modulation (PWM); STATCOM.

[*]Corresponding author: *e-mail*: vsuru@em.ucv.ro

1. Introduction

The control algorithm of the shunt active power filter uses two regulating loops: one for the compensating capacitor voltage and one for the desired current (Bitoleanu & Popescu, 2010). The latter gives two directions:

a) direct current control – the active filter controls the compensating current, generated to the point of common coupling (Popescu *et. al*. 2009);

b) indirect current control – the active filter controls the current absorbed from the power grid by the entire system consisting of the active filter and the nonlinear loads (Bitoleanu *et al*., 2016).

The compensating capacitor voltage controller is typically proportional-integrative and the current controllers can be (Suru *et al*., 2014):

a) proportional – integrative – which have the advantage of constant switching frequency and best performances with the cost of difficult parameter tuning and performance dependent on controlled system modification;

b) hysteresis type – which have the advantage of simplicity, robustness and no parameter tuning but with the cost of variable switching frequency.

The proposed constant switching frequency hysteresis controller combines the classical hysteresis with the PI regulating loop suboptimal PWM modulator. In theory this should give the hysteresis controller stated advantages combined with constant switching frequency.

After the introduction, in the second chapter of this paper, the shunt active filter regulating loops are described, for the adopted control method, for both, classical solution and proposed regulator. The constant switching hysteresis controller is substantiated and its implementation in the Matlab Simulink environment is described in the third chapter and in the fourth chapter the simulation results are presented. In the fifth chapter the control algorithm preparation for the experimental setup is described, using a dSpace DS1103 control and the sixth chapter contains the experimental results. Finally the conclusions are drawn in the last chapter.

2. The Constant Frequency Hysteresis Regulator

The shunt active filter closed loop control is illustrated in Fig. 1, considering the direct current control:

i) V_C – the compensating capacitor voltage;

ii) i_L – nonlinear load current;

iii) APF – active power filter;

iv) VT – voltage transducer.

This type of control, compared to the indirect current control, has the advantage that the compensation can be easily customized (for the indirect current control, the compensation is intrinsic, it cannot be disabled, and also, partial compensation cannot be obtained).

So, the compensating capacitor voltage loop generates only the current absorbed by the active filter to charge the compensating capacitor. This current is added (in fact, subtracted, because the power flow is in reverse) to the

computed compensating current. The resulting current is prescribed to the current loop which controls the current through the interface inductor, which is the current generated by the active filter to the point of common coupling (Bitoleanu *et al*., 2010).
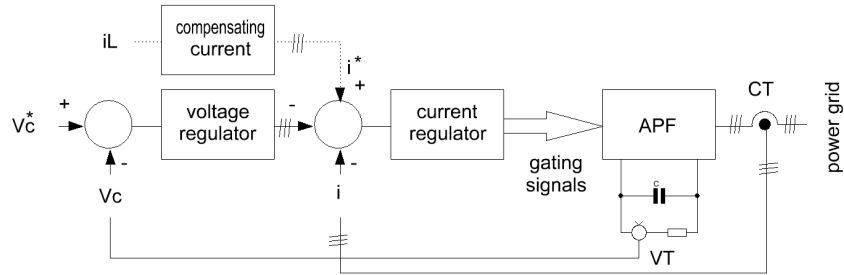

Fig. 1 – The active filter control algorithm based on direct current control.

The active filter IGBT gating signals are obtained by the classical hysteresis controller based on the error between the prescribed current and the output current (Fig. 2). The current error slides between the maximum and minimum value of the hysteresis band, when the output changes its state. In the interval between the limits, the regulator output (inverter gating signals) remains unchanged.
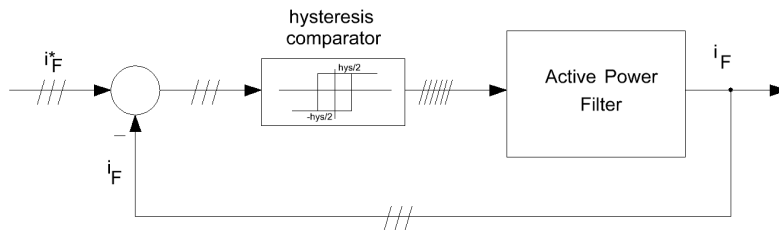

Fig. 2 – The current loop based on the classical hysteresis regulator.

The output current tracks the prescribed current within the constant hysteresis band, giving a variable switching frequency, dependent on the prescribed current rate of change – Fig. 3 (Buhler, 1986).
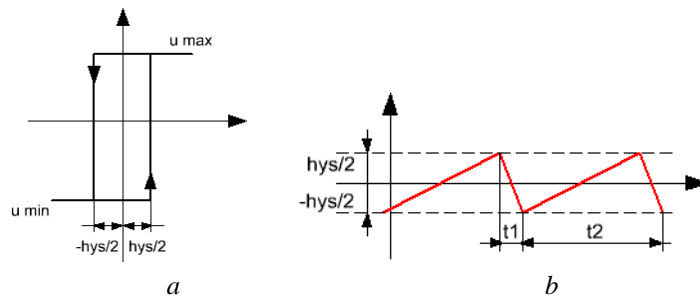

Fig. 3 – Classical hysteresis controller commutation law (*a*) and current shape (*b*).

The switching frequency is given by the current error time of change – Fig. 3 (Buhler, 1986):

$$f_{sw} = \frac{1}{t_1 + t_2},$$ (1)

where:

$$t_1 = \frac{hys}{u_{max} - u_{eq}},$$ (2)

and

$$t_2 = \frac{hys}{u_{eq} - u_{min}},$$ (3)

are the falling and rising times of the active filter current error. The quantities u_{max}, u_{min}, and u_{eq} are the maximum output, minimum output and the equivalent, average output of the active filter, which is the voltage between the power inverter output and the power grid (Buhler, 1986).

The average output of the active filter is defined as:

$$u_{eq} = \frac{R}{L} \cdot i_F + \frac{di_F}{dt}.$$ (4)

From (1) and (4) it results that the active filter switching frequency is dependent on the imposed hysteresis band, on the interface filter inductance, on the output current rate of change, and on the voltage across the interface filter (Buhler, 1986). The maximum switching frequency is reached when u_{eq} is null, and can be define as:

$$f_{swmax} = \frac{1}{4hys} \cdot \left(u_{max} - u_{min} \right).$$ (5)

On the other hand, the switching frequency reaches its minimum (it's actually canceled) when the equivalent output of active filter, u_{eq}, is equal to u_{max} or u_{min} (Buhler, 1986).

To obtain the constant switching frequency, the hysteresis controller error is over-modulated with an auxiliary triangular (or saw-tooth) signal, i_r – Fig. 4 (Buhler, 1986).

In this case, the switching moments aren't imposed by the current error (reaching the hysteresis band limits), but are determined by the intersection of the current error with the triangular carrier (Fig. 5). This means that the current error ripple is variable and dependent on the carrier frequency on one hand and on the current (error) rate of change, on the other hand.
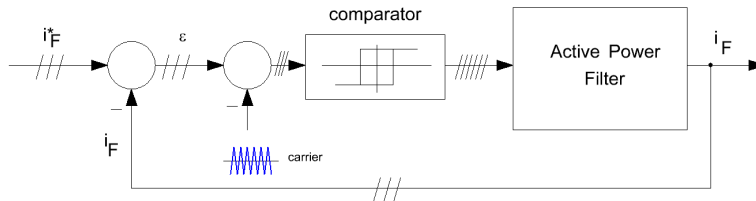
Fig. 4 − The current loop based on the constant switching
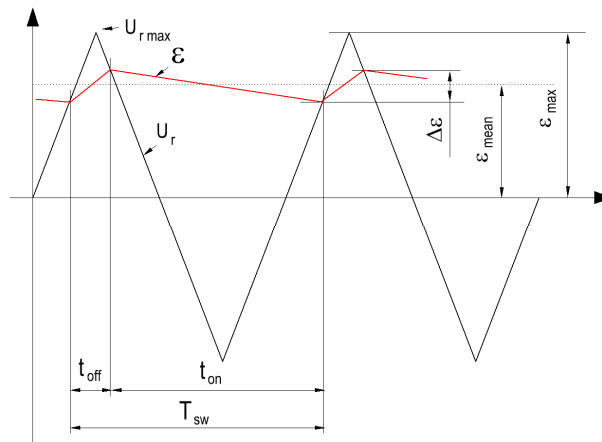frequency hysteresis regulator.

Fig. 5 – The PWM modulator input signals: the current error on the non-inverting input
and the triangular carrier on the inverting input.

In this case, the switching period is constant and defined as the sum of the transistor on and off time intervals (Buhler, 1986):

$$t_{on} = \frac{u_{eq} - u_{min}}{u_{max} - u_{min}} \cdot T_{sw},$$ (6)

$$t_{off} = \frac{u_{max} - u_{eq}}{u_{max} - u_{min}} \cdot T_{sw}.$$ (7)

It can be seen that the conduction time is maximum when the active filter equivalent output is maximum and minimum when the active filter equivalent output is minimum.

Regarding the current error, it also has an equivalent, average value, defined as (Buhler, 1986):

$$\varepsilon_{mean} = \frac{2u_{eq} - (u_{max} + u_{min})}{u_{max} - u_{min}} \cdot U_{rmax}$$ (8)

Therefore, it can be concluded that when u_{eq} varies between u_{min} and u_{max}, ε_{mean} varies between $- U_{r\,max}$ and $U_{r\,max}$.

Thus, for high current slope, the current error could exceed the carrier amplitude, and consequently, the active filter output will tend to exceed its limits, the filter being unable to obtain the prescribed current.
In order to function correctly, it is necessary that the carrier rate of rise is high enough, compared to current error (Buhler, 1986).

3. The Control Algorithm Implementation

The proposed constant switching frequency current controller was implemented in the Matlab Simulink environment, in a complete active filtering system.

The model contains the filtering system hardware components implemented with SimPowerSystems blocks and the corresponding control loops implemented in a distinct control block (Fig. 6).
The rated powers of the system components are (corresponding to the experimental setup rated powers):
- Active Power Filter:
   o UN = 380V, IN = 25A;
   o Compensating capacitor: 1100 µF;
   o Interface filter: 4.4 mH;
- Nonlinear Load:
   o UN = 380V, IN = 15A;
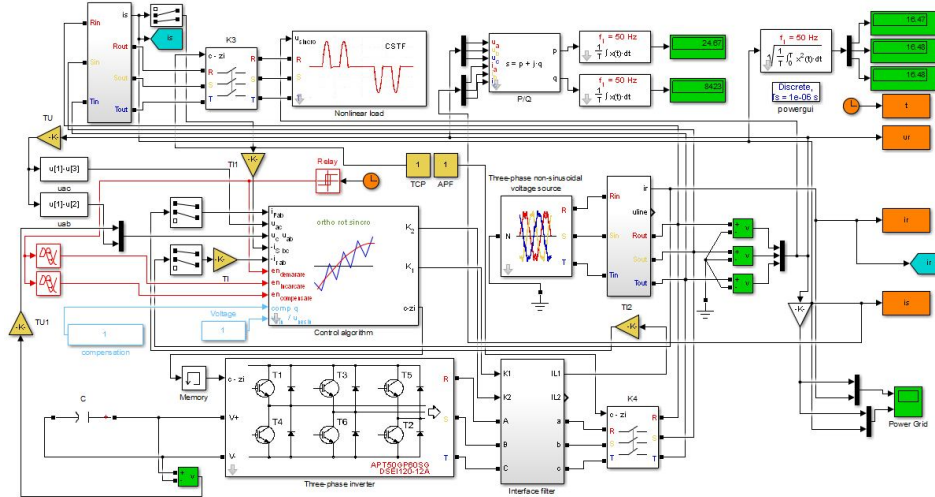   o SN = 9 kVA, QN = 9 kvar.

Fig. 6 – The Simulink model of the active filtering system (power and control section).

The nonlinear load Simulink block was created as the virtual model of the experimental laboratory load. This load, made by Nokian Capacitors has the purpose to absorb a distorted and reactive current similar in shape to the current absorbed by the AC drive systems. The particularity of this laboratory converter is that is absorbs only reactive and distortion power, it absorbs in theory no active power.

In order to validate the correct behavior of the active filtering system model and to compare the obtained performance, the model in Fig. 6 was first implemented with a classical hysteresis controller (Fig. 7 *a*). The hysteresis band was chosen to 2.5% of the rated current, which is about 60 mA. In a copy of the Simulink model (in Fig. 6), the constant switching frequency controller replaced the classical hysteresis one (the carrier frequency was set to 20 kHz with unitary amplitude).

Because the compensating capacitor voltage regulator is normalized, the nominal voltage was considered 800 V. Also, the maximum input value was set to 10 (because the current loop is not normalized, the voltage regulator output limit is 25 A.

The active filter uses the direct current control, so the compensating current must be computed – the adopted decomposition method was the synchronous rotating d-q frame (Asiminoaei *et al*., 2005; Miranda *et al*., 2005; Popescu *et al*., 2015; Suru *et al*., 2014).
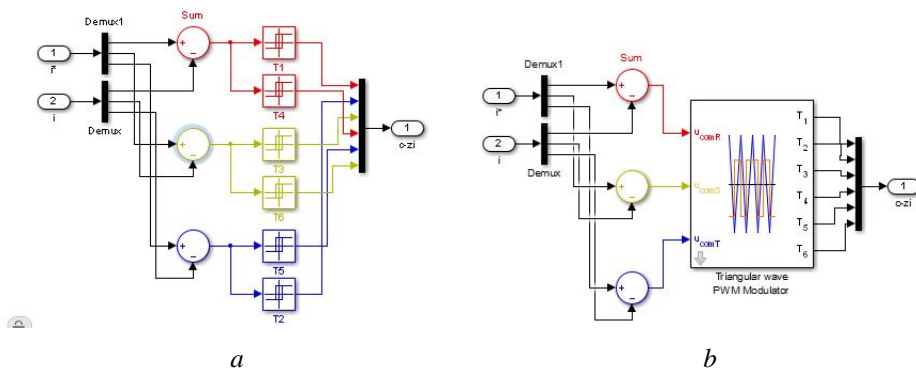

| *a* | *b* |

Fig. 7 – The classical hysteresis regulator (*a*) and the constant switching frequency regulator (*b*).

4. The Simulation Results

The simulation results obtained with the model in Fig. 6 for the current regulators in Fig 7 were analysed in steady state operation (the active filter compensating capacitor is charged at 700 V and the compensation is validated).

For both controllers, the nonlinear load current absorbed from the point of common coupling is illustrated in Fig. 8 *a*, and the corresponding harmonic spectra in Fig. 8 *b*.

The total harmonic distortion factor of this current is 77.30% for a RMS value of 16.47 A. The active power absorbed by the nonlinear load is 24.67 W, and the reactive power is 8.42 kvar.
The total harmonic distortion factor of the grid voltage is 3.04%.

The power grid current waveform, obtained after compensation with the classical hysteresis regulator is illustrated in Fig. 9 *a*, and the corresponding harmonic spectra in Fig. 9 *b*.

The total harmonic distortion factor is 2%, giving a filtering efficiency of 38.70. Considering the partial harmonic distortion factor (for the first 51 harmonics) it results a value of 1.86%, giving a filtering efficiency of 41.47, which is not very different. This means that the majority of the harmonics are below the 51th, so the active filter switching operation does not generate the most important harmonics (for a simulation time step of 1 μs) compared to the ones generated by the compensation algorithm limitation.
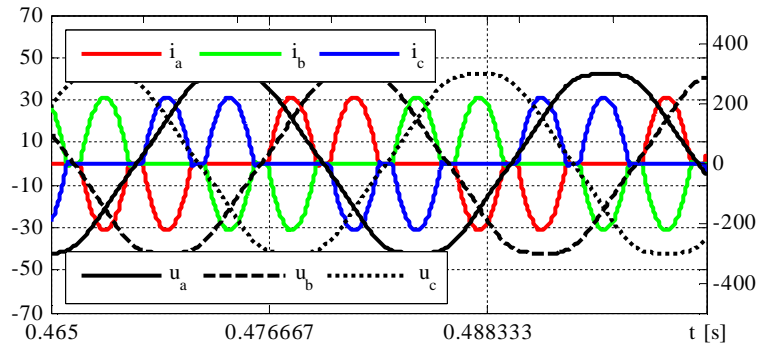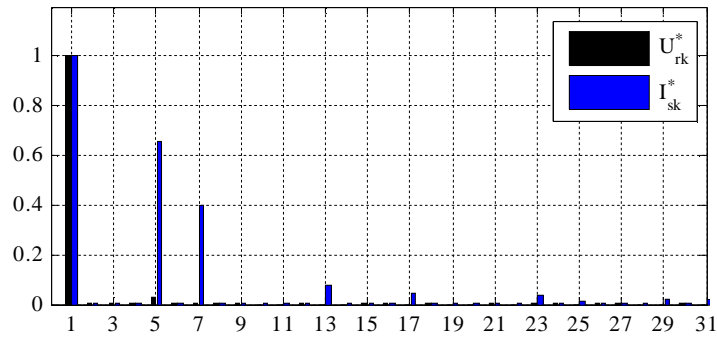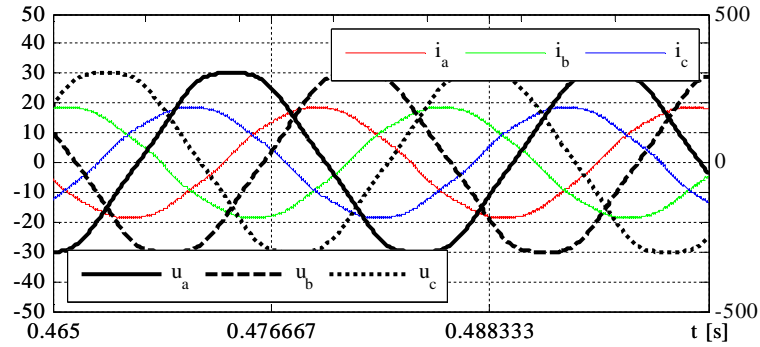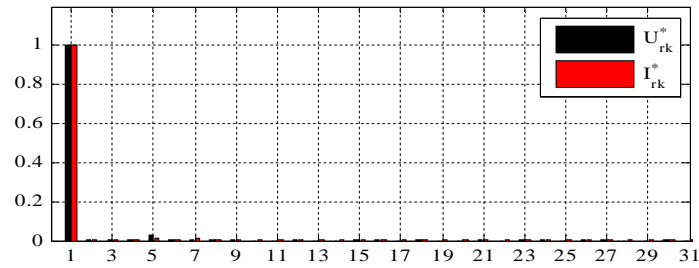

a

b

Fig. 8 – The power grid voltage and nonlinear load current:
a – waveforms; *b* – harmonic spectra.
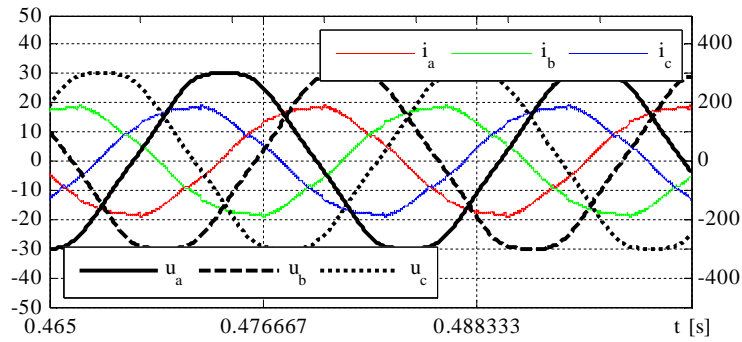
The compensation result obtained with the constant switching frequency current regulator is illustrated in Fig. 9 *c* and *d*.
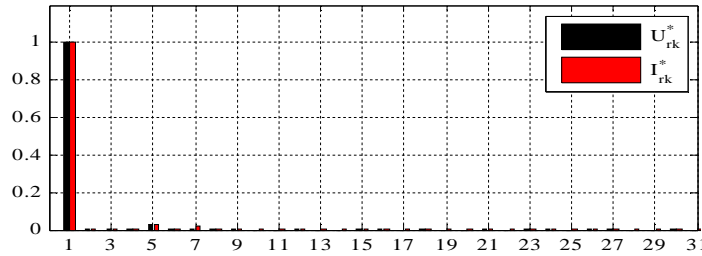
Fig. 9 – The compensated power grid current for: the classical hysteresis controller, waveform (*a*) and harmonic spectra (*b*), the constant switching frequency hysteresis controller, waveform (*c*) and harmonic spectra (*d*).

It can be seen that the compensated current waveform has a little more distortion, the total harmonic distortion factor being 3.80% (the filtering efficiency in this case is about half, 20.36). The partial harmonic distortion factor (51 harmonics) is 3.43% which again, means that the majority of the harmonics are low order. Although, the current ripple in this case is higher because the switching frequency is fixed at 20 kHz (the maximum switching frequency for the active filtering system parameters with the classical controller is as high as 167 kHz).

In order to explain the two controllers behavior, the compensating current is illustrated in Fig 10 *a* for the hysteresis regulator and in Fig. 10 *b* for the constant switching frequency hysteresis regulator. It results that the constant switching frequency controller has a slight lag following the prescribed current, giving the higher distortion of the compensated current.
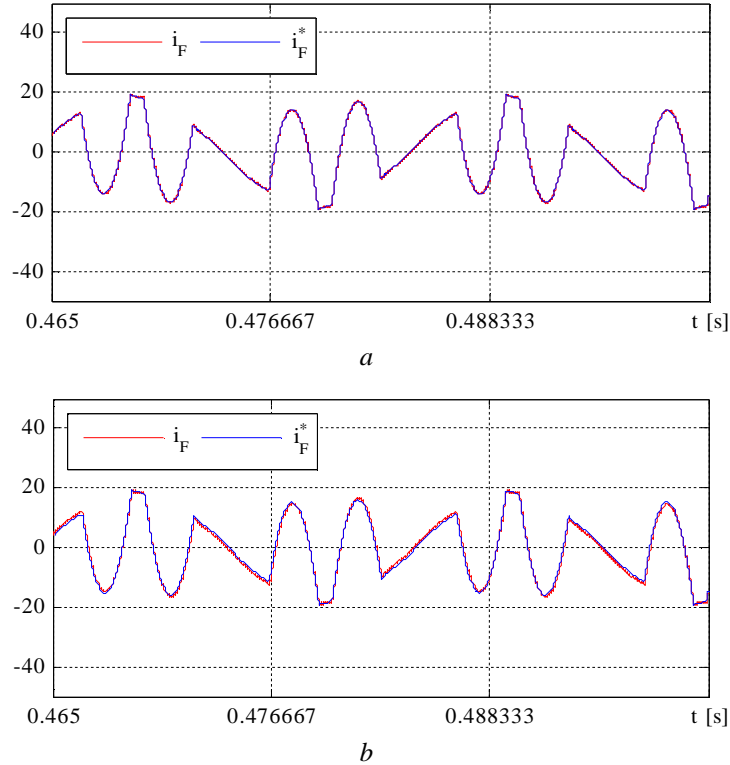

a

b

Fig. 10 – The active filter output current and prescribed current for the: *a* – classical hysteresis controller; *b* – constant switching frequency hysteresis controller.

To make a comparison between the two controllers principle of operation, the current error for the both controllers is illustrated in Fig. 11. It results that in the case of the classical controller, the hysteresis band is exceeded because of the simulation step of 1 μs (the imposed band is about

60 mA). Although, the resulting band is maintained relatively constant at about 360 mA (excepting the filter current zero crossings, when it is 577 mA). This behavior is getting worse with the increase of the simulation step.

For the constant switching frequency controller (Fig. 11 *b*), it must be mentioned that the carrier amplitude is unitary, therefore, there are several moments when the current error exceeds the carrier amplitude. This is affecting the switching frequency because the time interval the current error is higher than the carrier amplitude the gating signal is not changed so the switching frequency is lower than the carrier frequency.
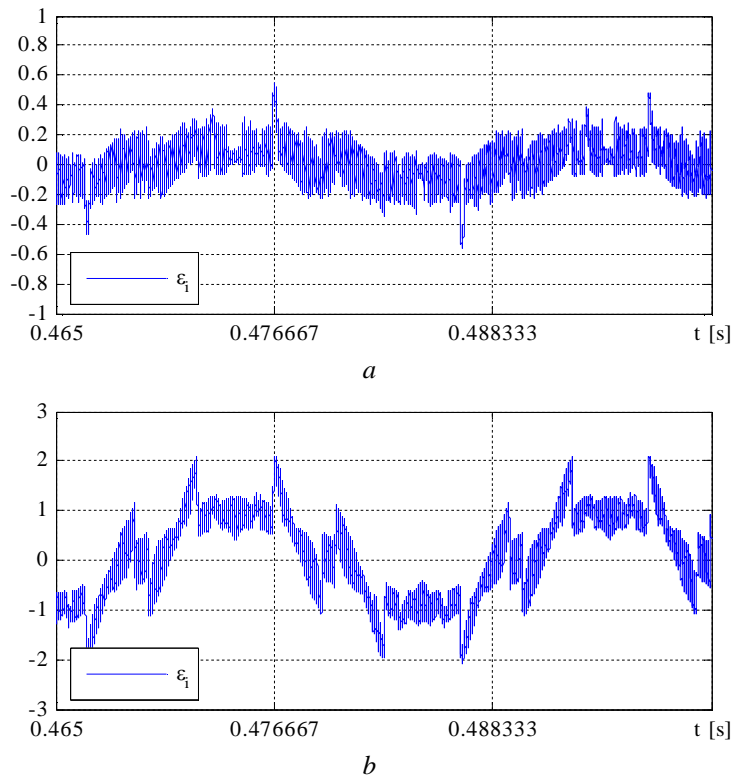

a

b

Fig. 11 – The current error for the: *a* – classical hysteresis controller; *b* – constant switching frequency hysteresis controller.

This can be observed in Fig. 12 *b*, where on each time interval the carrier is exceeded, the virtually measured switching frequency drops (the longer is the time interval, the more the switching frequency decreases.

This can be due to the fact that when the average output of the active filter u_{eq} varies between u_{max} and u_{min}, the average value of the current error varies between the positive and negative amplitude of the carrier signal (Bitoleanu *et al*., 2016). If the current error exceeds the carrier amplitude, then not

only the switching frequency drops, but the active filter average output reaches u_{max} or u_{min}, being impossible for the active filter output current to follow the prescribed current (this can be observed in Fig 10 *b*, compared to Fig. 10 *a*).

For comparison, the classical hysteresis controller switching frequency is plotted in Fig. 12 *a*. It results that the switching frequency varies between 795 Hz and 167 kHz.
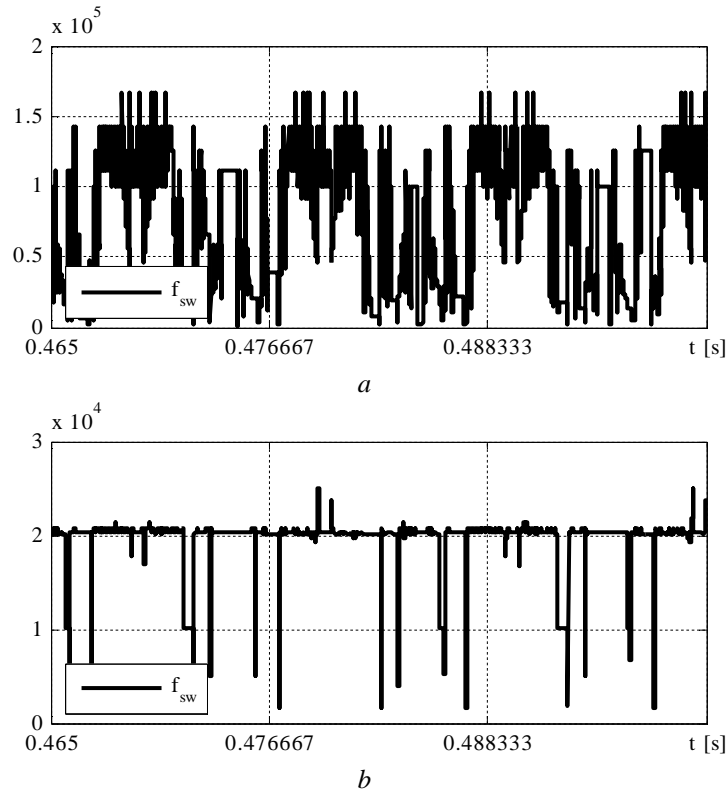

a

b

Fig. 12 – The active filter switching frequency for the: *a* – classical hysteresis controller; *b* – constant switching frequency hysteresis controller.

5. The Experimental Setup

The studies completed on the model in Fig. 6 were experimentally tested on an experimental model of the active filtering system containing the same components as the virtual system, with the same rated values.
To validate the proposed current controller, the active filter control algorithm Simulink block (Fig. 6) was exported to control the experimental active filter by means of a dSpace DS1103 control board. To do this, al the SimScape/ SimPowerSystems blocks corresponding to the virtual power section of the active filtering system in Fig 6 were deleted and replaced with DS1103 RTI (Real Time Interface) blocks (Suru *et al.*, 2013).

These blocks are necessary for the control algorithm inputs and outputs to the real system:

– analog to digital converters – receiving the analog signals from the system current and voltage transducers;

– digital outputs – the gating signals generated by the control algorithm are applied to the power inverter by means of the corresponding interface circuits.

The same comparison was made between the results obtained by the proposed constant switching hysteresis controller and the results obtained with the classical hysteresis controller.

It must be mentioned that for the classical hysteresis controller, the gating signals were generated by software (Simulink model) and given to the power inverter by means of the digital I/O ports of the DS1103 board (Fig. 13 *a*).

For the case of the constant switching frequency hysteresis controller, the PWM modulator is necessary and the 20 kHz carrier waveform is not possible to be obtained at the simulation time step of the DS1103 (of about 20 μs). To overcome this, only the current error was computed in the Simulink model (Fig. 7 *b*) and the integrated hardware PWM modulator of the DS1103 was used (Fig. 13 *b*).

For both controllers, the experimental control algorithm (illustrated in Fig. 13) was compiled and loaded to the DS1103 program memory.
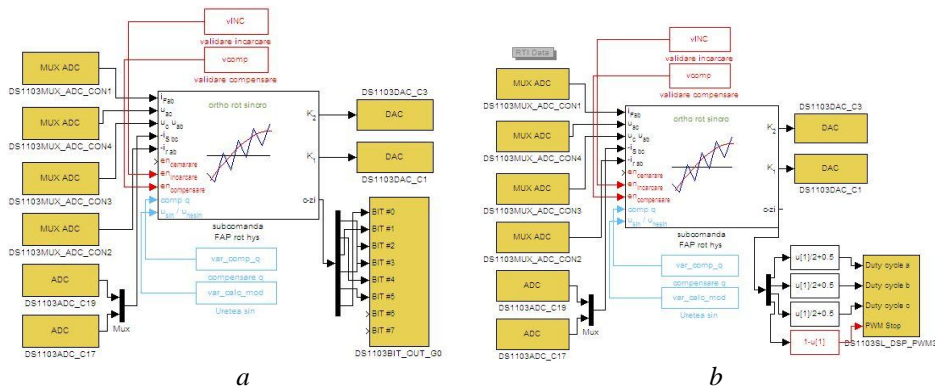

Fig. 13 – The control algorithm based on the classical hysteresis regulator (*a*) and on the constant switching frequency regulator (*b*).

The real time control and monitoring of the experimental active filter was done using a virtual control panel, created in ControlDesk (the DS1103 dedicated control software (Fig. 14)).

Because all the signals in the control Simulink model can be sampled and saved as a Matlab structure, the power grid voltages and currents could be plotted and numerically analyzed in Matlab/Simulink. The nonlinear load current and the compensated grid current were also captured using a Metrix OX704M digital oscilloscope (Fig. 15).

For both controllers, the nonlinear load current absorbed from the point of common coupling is illustrated in Fig. 15 and the corresponding harmonic spectra in Fig. 16.
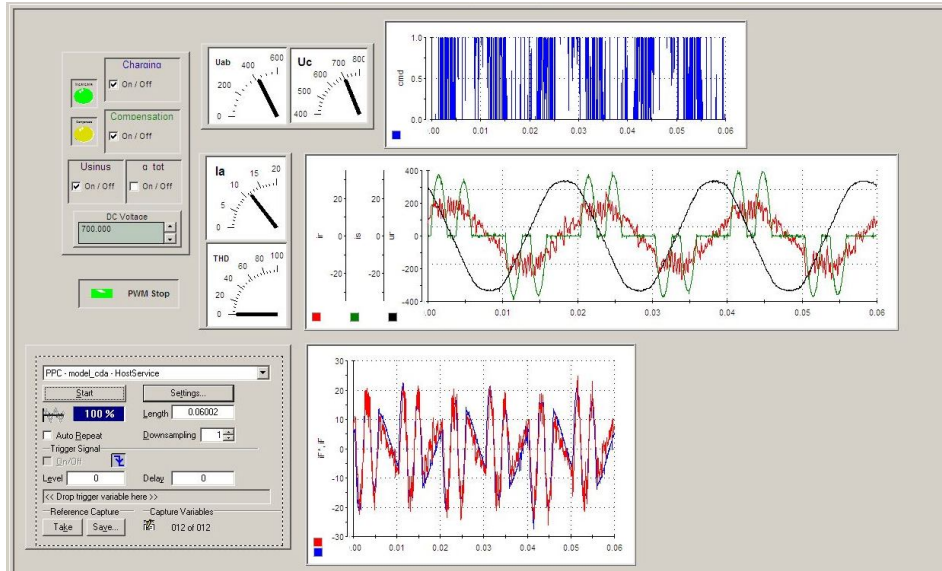

Fig. 14 – The virtual control panel of the experimental active filter.

The total harmonic distortion factor of this current is 92.69% for a RMS value of 15.43 A. The total harmonic distortion factor of the grid voltage at the experiment time is 2.65%.

The power grid current waveform, obtained after compensation with the classical hysteresis regulator is illustrated in Fig. 15 *a*. The total harmonic distortion factor is 12.62%, giving a filtering efficiency of 7.34. The performance of the experimental active filter is lower than the performance obtained by simulation mainly because of the simulation step which is considerably higher in this case (23 μs as of 1μs). For the DS1103 program obtained by compiling the Simulink model in Fig. 13, the simulation time step is the real time step. This causes the generated gating signal to switch on or off after this large time step, causing the real switching frequency to be lower than the necessary frequency (the switching frequency varies between 745 Hz 22 kHz). This also leads to a hysteresis band considerably larger due to current overshoot (the experimental resulted hysteresis band is as high as 3.84 A)

The power grid current waveform, obtained after compensation with the constant switching frequency hysteresis regulator is illustrated in Fig. 15 *b*. The total harmonic distortion factor is 29.39%, giving a filtering efficiency of 3.08. The performance of the experimental active filter is considerably lower than the performance obtained by simulation, yet again, because of the simulation step (20 μs as of 1μs), but also, lower than the classical hysteresis controller

performance. To find out why, the active filter current for the two cases is illustrated in Fig. 17.
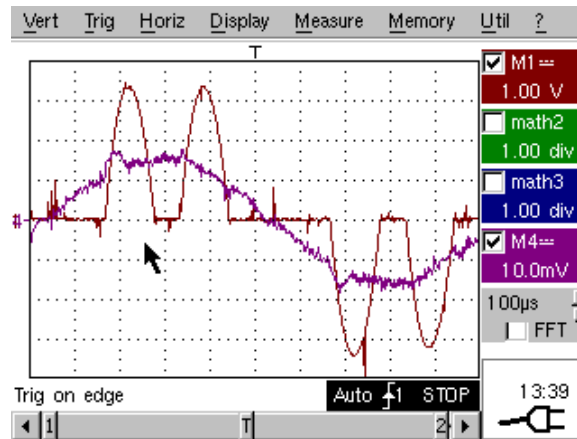
a
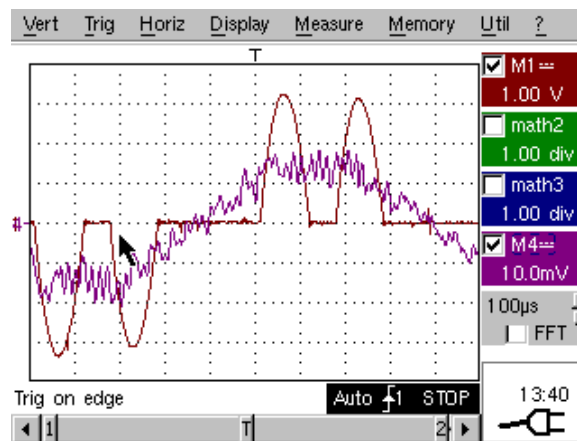
b

Fig. 15 – The experimental nonlinear load current (M1) and the compensated power grid current (M4) for: *a* – the classical hysteresis controller; *b* – the constant switching frequency hysteresis controller.
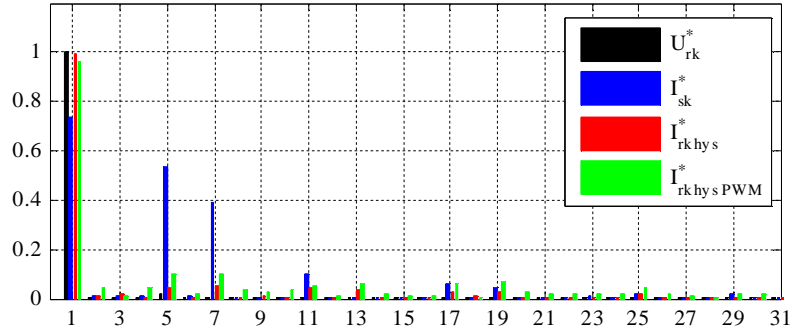
Fig. 16 – The harmonic spectra for the power grid voltage, nonlinear load current and compensated grid current for the investigated current controllers.

It can be seen that the filter current is far from the desired waveform, with high ripple (which cannot be at 20 kHz) and visible variable switching frequency. Because the PWM modulator which was used is integrated in the DS1103 hardware, the carrier shape could not be affected by the time step of 20 μs.
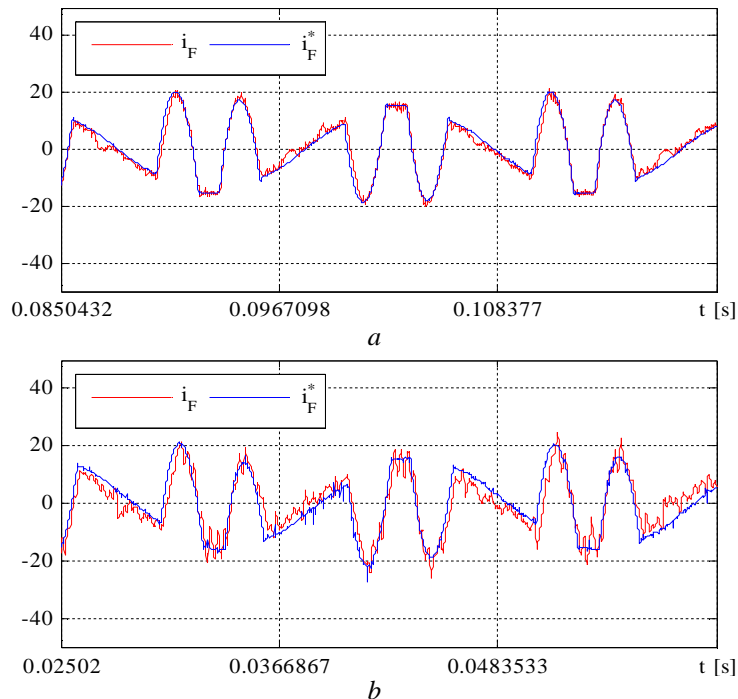

Fig. 17 – The experimental active filter output current and prescribed current for the: *a* – classical hysteresis controller; *b* – constant switching frequency hysteresis controller.

The current error, illustrated in Fig. 18, gives the explication: because of the time step, the control algorithm response is delayed – the current error instantaneous value applied to the PWM modulator is updated once every 20 μs.

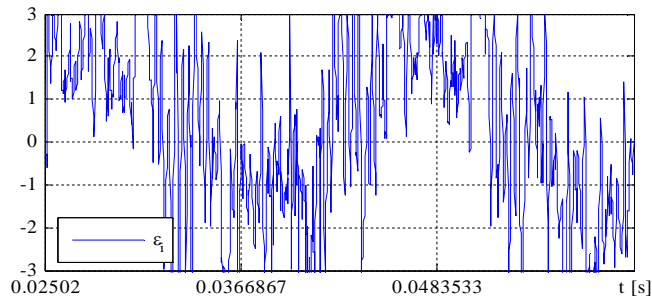Fig. 18 – The experimental active filter current error applied to the PWM modulator.
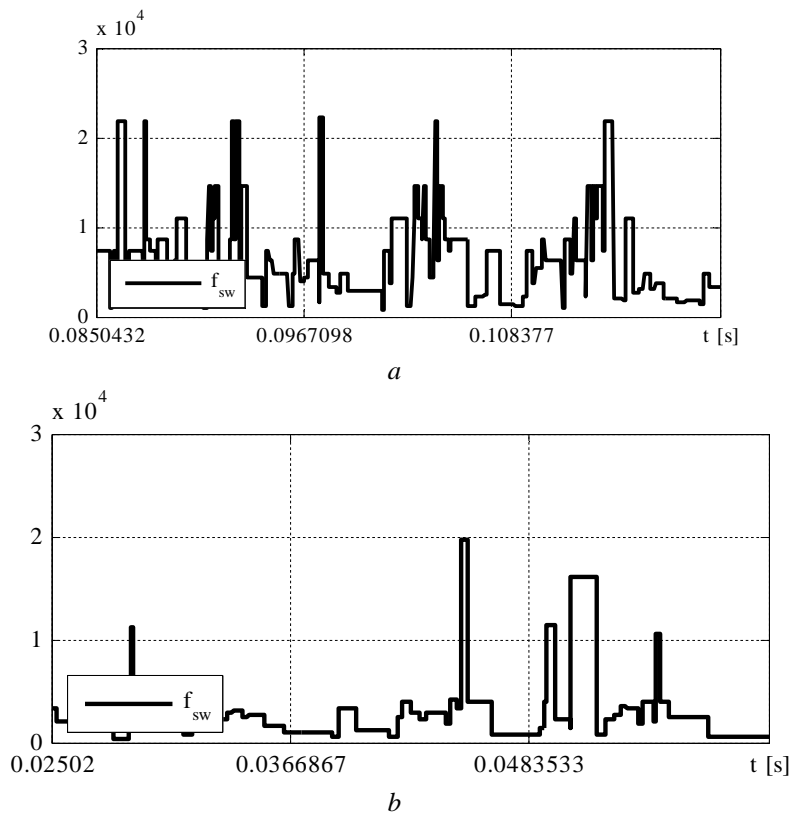

a

b

Fig. 19 – The experimental active filter switching frequency for the: *a* – classical hysteresis controller; *b* – constant switching frequency hysteresis controller.

In this time interval, the current error applied to the modulator keeps its computed value while the real current error is constantly increasing; causing the

filter current to overshoot in a similar manner it does in the case of the classical hysteresis controller. The difference is that in this case, the current error gets as high as 6.78 for unitary carrier amplitude so the generated gating signals are highly saturated. The effect can be seen in Fig. 19 *b*, where the switching frequency should vary between 369 Hz and 143 kHz, if only the sampled current error and the triangular carrier were taken into consideration. In the experimental setup, the gating signals generated at the output of the PWM modulator are applied to the IGBT's with an imposed dead-time of about 50 μs so the real switching frequency varies between 358 Hz and 19.67 kHz.

However, the switching frequency is not constant and as a rule, it keeps bellow 5 kHz. This causes the distortion of the active filter output current (Fig. 17 *b*).

6. Conclusions

After a comprehensive analysis of the constant switching frequency hysteresis controller, the validity of this concept has been proven. Despite the fact that the proposed current regulator introduces a slight delay between the prescribed current and the output current, and also, the compensated current has little more distortion compared to the results obtained with the classical regulators, the results are sufficiently good to make this regulator a valid alternative. This is because although the performances are a little lower, the regulator is simple, no tuning is required, and the constant switching frequency is achieved.

The different performance obtained by this regulator by simulation combined with the experimental results prove the fact that, the same as the PI regulator, the proposed regulator needs higher computational power compared with the classical hysteresis controller. The latter simply obtains lower performances as the computational power decreases, but the first two are becoming unstable and their performances drops if the time step is not low enough.

REFERENCES

Asiminoaei L., Blaabjerg F., Hansen S., *Evaluation of Harmonic Detection Methods for Active Power Filter Applications*, Applied Power Electronics Conf. and Exposition, 2005, 635-641.
Bina M. T., Pashajavid E., *An Efficient Procedure to Design Passive LCL-filters for Active Power Filters*, Electric Power Systems Research, **79**, 606–614 (2009).
Bitoleanu A., Popescu M., Suru V., *Optimal Controllers Design in Indirect Current Control System of Active DC-Traction Substation*, 17th IEEE Internat. Power Electronics and Motion Control Conf. (PEMC) Varna, Bulgaria, Sep 25-28, 2016, 2016 Book Series: IEEE Internat. Power Electronics and Motion Control Conf. IPEMC, 2016, 912-917.
Bitoleanu A., Popescu Mh., *Filtre Active de Putere*, Ed. Universitaria, Craiova, 2010.
Buhler H, *Réglage par mode de glissement*, Presses Polytechniques Romandes, 1986.

Chang G.W., Tai-Chang S., *A Comparative Study of Active Power Filter Reference Compensation Approaches*, Proc. of Power Engineering Society, **2**, 1017-1021 (2002).

Ingram D., Round S., *A Fully Digital Hysteresis Current Controller for an Active Power Filter*, Internat. J. of Electronics, **86** (1999.)

Miranda U.A., Rolim R.G.B., Aredes M., *A DQ Synchronous Reference Frame Control for Single-Phase Converters*, Power Electronics Specialists Conf., 2005, 1377-1381.

Patjoshi R.K., Mahapatra K.K, *Performance Comparison of Direct and Indirect Current Control Techniques Applied to a Sliding Mode Based Shunt Active Power Filter*, India Conf. (INDICON), 2013 Annual IEEE, 1-5.

Popescu M., Bitoleanu A., Suru V*., Indirect Current Control in Active DC Railway Traction Substations*, 2015 Intl Aegean Conf. on Electrical Machines & Power Electronics (ACEMP), 2015 Intl Conf. on Optimization of Electrical & Electronic Equipment (OPTIM) & 2015 Intl Symp. on Advanced Electromechanical Motion Systems (ELECTROMOTION), 2015.

Popescu M., Preda A., Suru V., *Synchronous Reference Frame Method Applied in the Indirect Current Control for Active DC Traction Substation*, Athens: ATINER'S Conf. Paper Series, No: TRA2015-1552, 2015, 8-11 June, 2015, 1-6.

Popescu Mh., Bitoleanu A., Dobriceanu M., Linca M., *On the Cascade Control System Tuning for Shunt Active Filters Based on Modulus Optimum Criterion*, Circuit Theory and Design, 2009, ECCTD 2009, 23-27 Aug. 2009, 137-140.

Popescu Mh., Bitoleanu A., Dobriceanu M., Suru V., *Optimum Control Strategy of Three-Phase Shunt Active Filter System*, Proc.of World Academy of Science, Engineering and Technology, **58**, October 2009.

Suru C.V., Linca M, Patrascu CA, *Evaluation of Current Control Methods in Three-Phase Shunt Active Power Filters System*, Analele Universitatii Eftimie Murgu Resita Fascicola de Inginerie, **XXI**, *3*, 177-188 (2014).

Suru C.V., Patrascu C.A., Linca M., *The Synchronous Fundamental dq Frame Theory Implementation and Adaptation for the Active Filtering*, Internat. Conf. on Applied and Theoretical Electricity (ICATE), OCT 23-25, 2014.

Suru C.V., Popescu M., Pătrașcu A., *Using dSPACE in the Shunt Static Compensators Control,* Annals of The University of Craiova, **37**, 94-99 (2013) .

IMPLEMENTAREA UNUI REGULATOR DE CURENT CU HISTEREZIS CU
FRECVENȚA CONSTANTĂ PENTRU SISTEME DE FILTRARE ACTIVĂ

(Rezumat)

Lucrarea are ca scop implementarea și validarea unui regulator de curent cu histerezis cu frecvență constantă de comutație. Acest tip de regulator poate fi o alternativă atât pentru clasicul regulator cu histerezis, cât și pentru regulatorul PI, deoarece permite obținerea semnalelor de comandă cu frecvență constantă specifice regulatorului de tip PI cu modulator PWM și simplitatea și robustețea specifice regulatorului cu histerezis. Regulatorul cu histerezis propus reprezintă un compromis între cele două soluții clasice. Poate fi obținut practic prin combinarea comparatoarelor regulatorului cu histerezis cu modulatorul PWM din componența sistemului de reglare cu regulator PI.

Pe de altă parte, atât rezultatele obținute prin simulare cât și cele experimentale, sunt mai puțin bune decât cele obținute cu soluțiile clasice. Mai exact, rezultatele obținute depind de parametrii regulatorului tensiunii pe condensatorul de compensare respectiv, de valoarea acestei tensiuni. A fost confirmat faptul că la utilizarea regulatorului propus, invertorul lucrează cu frecvență constantă de comutație, dar este introdusă o întârziere între forma de undă a curentului compensator prescris și forma de undă a curentului compensator real. Implementarea acestui tip de regulator a fost studiată atât prin simulare, într-un model complet al sistemului de filtrare activă, realizat în Matlab Simulink, cât și pe un sistem de filtrare experimental comandat cu ajutorul unei plăci de comandă dSpace DS11034.